

The Arabidopsis eukaryotic translation initiation factor 3, subunit F (*AtelF3f*), is required for pollen germination and embryogenesis

Chuan Xia¹, Yu-Jiao Wang¹, Wen-Qing Li¹, Yi-Ran Chen¹, Yi Deng¹, Xue-Qin Zhang¹, Li-Qun Chen¹ and De Ye^{1,2,*}

¹State Key Laboratory of Plant Physiology and Biochemistry, College of Biological Sciences, China Agricultural University, Beijing 100193, China, and

²National Center for Plant Gene Research (Beijing), Beijing 100101, China

Received 8 February 2010; revised 2 April 2010; accepted 9 April 2010; published online 26 May 2010.

*For correspondence (fax +86 10 62734839; e-mail yede@cau.edu.cn).

SUMMARY

Previous studies have shown that subunits E (eIF3e), F (eIF3f) and H (eIF3h) of eukaryotic translation initiation factor 3 play important roles in cell development in humans and yeast. eIF3e and eIF3h have also been reported to be important for normal cell growth in Arabidopsis. However, the functions of subunit eIF3f remain largely unknown in plant species. Here we report characterization of mutants for the Arabidopsis *eIF3f* (*AtelF3f*) gene. *AtelF3f* encodes a protein that is highly expressed in pollen grains, developing embryos and root tips, and interacts with Arabidopsis eIF3e and eIF3h proteins. A *Ds* insertional mutation in *AtelF3f* disrupted pollen germination and embryo development. Expression of some of the genes that are essential for pollen tube growth and embryogenesis is down-regulated in *ateif3f-1* homozygous seedlings obtained by pollen rescue. These results suggested that *AtelF3f* might play important roles in Arabidopsis cell growth and differentiation in combination with eIF3e and eIF3h.

Keywords: *AtelF3f*, translation initiation, MPN domain, male gametophyte, embryogenesis, Arabidopsis.

INTRODUCTION

In higher plants, pollen tube elongation in the pistil is a crucial step for sexual reproduction. Many important biological processes are involved. For example, a tip-focused calcium gradient plays a central role in orienting tip growth (Dumas and Gaude, 2006). Cell wall-modifying enzymes are required for normal pollen tube elongation (Krichevsky *et al.*, 2007). Exocytosis is also one of the major processes responsible for polarized cell growth (Malho *et al.*, 2006). To carry out these biological processes, numerous proteins need to be synthesized precisely during pollen tube growth and elongation.

In protein synthesis processes, mRNA translation is regulated at both global and message-specific levels, especially at the step of translation initiation. The normal initiation of eukaryotic protein synthesis is facilitated by at least 12 eukaryotic translation initiation factors (eIFs), several of which are multiprotein complexes. The largest, eukaryotic translation initiation factor 3 (eIF3) (approximately 650 kDa), participates in most translation initiation processes (Asano *et al.*, 1997a; Sonenberg *et al.*, 2000; Kawaguchi and Bailey-Serres, 2002). eIF3 helps to maintain

the 40S and 60S ribosomal subunits in a dissociated state, and stabilizes binding of the eIF2-GTP-Met-tRNAi^{Met} ternary complex to the 40S subunit (Chaudhuri *et al.*, 1999; Sonenberg *et al.*, 2000). It promotes binding of the 43S pre-initiation complex to the 5' end of mRNA (Kolupaeva *et al.*, 2005; Hinnebusch, 2006). Moreover, it also plays roles in scanning for and recognizing AUG start codons (Lukaszewicz *et al.*, 2000; Dever, 2002; Nielsen *et al.*, 2004; Valasek *et al.*, 2004).

The components of eIF3 have been identified in many species. In humans, the functional core of eIF3 is made up of six (eIF3a, eIF3b, eIF3c, eIF3e, eIF3f, eIF3h) of 11 subunits. These are conserved in mammals, *Triticum aestivum* (wheat), *Arabidopsis thaliana*, *Saccharomyces pombe* and *Drosophila melanogaster* (Asano *et al.*, 1997b; Burks *et al.*, 2001; Masutani *et al.*, 2007; Zhou *et al.*, 2008). However, only eIF3a, eIF3b and eIF3c are found in the eIF3 core of *Saccharomyces cerevisiae*, which has five subunits (eIF3a, eIF3b, eIF3c, eIF3g and eIF3i), indicating that eIF3e, eIF3f and eIF3h may not be necessary for global translation initiation (Asano *et al.*, 1998; Burks *et al.*, 2001; Zhou *et al.*, 2005).

eIF3e and eIF3h are not essential for global translation initiation in fission yeast, but their knockout affects spore formation, indicating that they may have special roles in cell differentiation (Bandyopadhyay *et al.*, 2000; Zhou *et al.*, 2005; Ray *et al.*, 2008). eIF3f is down-regulated in many human tumours, and over-expression of eIF3f inhibits cell proliferation and induces apoptosis in tumour cells (Shi *et al.*, 2006; Doldan *et al.*, 2008a,b). These results suggest that eIF3e, eIF3f and eIF3h play important roles in the normal growth of human and yeast cells but are not necessary for global translation initiation.

In Arabidopsis, deletion of the *eIF3e* gene (*AtelF3e*) results in male gametophytic lethality in the *eIF3e-Tnull* mutant (Yahalom *et al.*, 2008), indicating that it is required for male gametogenesis. Over-expression of eIF3e affects seed formation (Yahalom *et al.*, 2008). Therefore, eIF3e plays roles in Arabidopsis embryogenesis. Mutation of the Arabidopsis *eIF3h* gene not only significantly reduced Arabidopsis fertility, but also resulted in hypersensitivity of *eif3h-1* mutant seedlings to exogenous sugars (Kim *et al.*, 2004, 2007). In summary, eIF3e and eIF3h are important for normal plant cell growth. However, the roles of subunit eIF3f are largely unknown in plant species.

Here, we report the characterization of a male gametophyte-defective mutant generated by insertion of the transposon element *Ds* in *At2g39990*. As the *At2g39990* protein was identified in the Arabidopsis eIF3 complex and has high similarities to the eIF3f proteins found in many species (Burks *et al.*, 2001), we named the gene *Arabidopsis thaliana eIF3f* (*AtelF3f*), and the mutant alleles used in this study were named *ateif3f-1* and *ateif3f-2*. *AtelF3f* was highly expressed in pollen grains, pollen tubes, embryos and root tips, and was also constitutively expressed in other tissues. In a pollen rescue experiment, we found that the mutation in *AtelF3f* also led to defects in embryogenesis. Further transcriptome analysis using *ateif3f-1* homozygous seedlings generated by pollen rescue showed that *AtelF3f* affected the expression of genes that are essential for pollen tube growth and embryogenesis, for example *AtCSLA7* (Goubet *et al.*, 2003). We also demonstrated that *AtelF3f* interacts with Arabidopsis eIF3e and eIF3h. These results suggest that eIF3f may play important roles in plant cell growth in combination with eIF3e and eIF3h in Arabidopsis.

RESULTS

Isolation and genetic analysis of the *ateif3f-1* mutant

The *ateif3f-1* mutant was isolated in a genetic screen for male gametophyte-defective mutants of a collection of gene-trap and enhancer-trap *Ds* insertion lines in Arabidopsis ecotype Landsberg *erecta* (*Ler*) (Sundaresan *et al.*, 1995). The *Ds* insertion created a genetic tag of kanamycin resistance in the mutant plant and a GUS reporter that was expressed specifically in pollen grains (see Figure S1a,b).

We first performed a genetic analysis of the *ateif3f-1* mutant (Table 1). The progeny from self-crossed *ateif3f-1/+* plants exhibited a segregation ratio of approximately 1:1 kanamycin-resistant (Kan^R):kanamycin-sensitive (Kan^S) (2116:2202), rather than the typical Mendelian segregation ratio of 3:1, and no Kan^R homozygous plants were identified in the progeny. This result indicates that the mutant is defective in gametophytic function.

To determine how the mutation affected male or female gametophytic functions, *ateif3f-1/+* plants were used as males or females in crosses with wild-type plants. As shown in Table 1, when the *ateif3f-1/+* plants were used as female parents, 49.2% (766/1558) of the resulting F₁ progeny were Kan^R. In contrast, when *ateif3f-1/+* pollen grains were used to pollinate wild-type plants, only 3.76% (61/1621) of the F₁ progeny were Kan^R. Thus the *ateif3f-1* mutation apparently drastically affected male gametophytic function and had little influence on female gametophytic function.

The *ateif3f-1* mutant is defective in pollen germination

To investigate how *ateif3f-1* affected male gametophytic function, we performed a quartet assay by introgression of the *ateif3f-1* mutation into the background of a *quartet1-2* (*qrt1-2*) mutant. The *qrt1-2* mutation blocks separation of the pollen grains from tetrads and has almost no effect on pollen tube growth (Preuss *et al.*, 1994). Therefore, a quartet from an *ateif3f-1/+ qrt1-2/qrt1-2* plant has two *ateif3f-1 qrt1-2* pollen grains (mutant) and two *qrt1-2* pollen grains (representing wild-type) derived from the same microsporocyte. We first stained the mature quartet pollen grains from *ateif3f-1/+ qrt1-2/qrt1-2* plants using 4',6-diamidino-2-phenylindole (DAPI). The *ateif3f-1 qrt1-2* pollen grains had two sperm nuclei and a vegetative nucleus like wild-type pollen grains and were morphologically normal. Therefore, the *ateif3f-1* mutation affected neither the formation of pollen nor its mitotic division (Figure 1a,b).

We examined germination of the pollen grains from *ateif3f-1/+ qrt1-2/qrt1-2* plants *in vitro*. Typically, the two *ateif3f-1 qrt1-2* mutant pollen grains did not germinate, but the two *qrt1-2* pollen grains (representing wild-type) did (Figure 1c). In the control, all four pollen grains germinated in an individual *qrt1-2* quartet (Figure 1d). Meanwhile, the

Table 1 Genetic analysis of the *ateif3f-1* mutant

Cross (female × male)	Number of Kan ^R seedlings	Number of Kan ^S seedlings	Kan ^R /Kan ^S ratio
<i>ateif3f-1/+ × atelF3f-1/+</i>	2116	2202	0.96
WT × <i>ateif3f-1/+</i>	61	1560	0.039
<i>ateif3f-1/+ × WT</i>	766	792	0.97

Kan^R, kanamycin-resistant; Kan^S, kanamycin-sensitive; WT, wild-type.

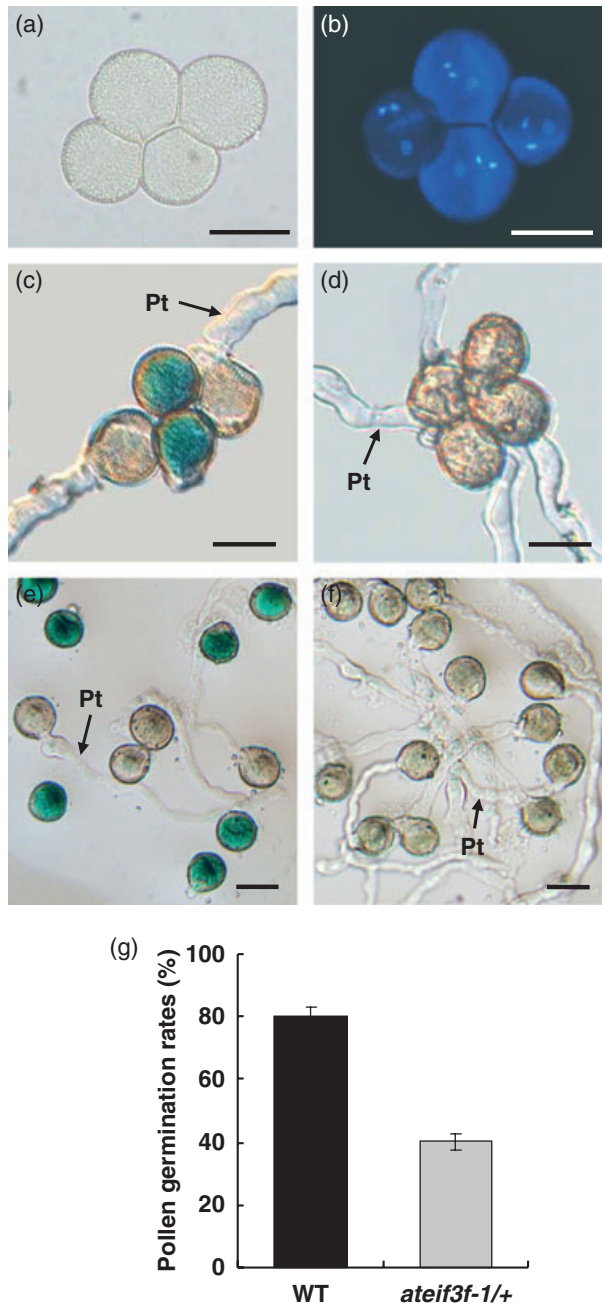


Figure 1. Characterization of *ateiF3f-1* mutant pollen. (a,b) DAPI-stained quartet pollen grains from *ateiF3f-1/+ qrt1-2/qrt1-2* plants in light field (a) and under UV light (b). (c–f) *In vitro* germination of pollen grains from *ateiF3f-1/+ qrt1-2/qrt1-2* plants (c), *qrt1-2/qrt1-2* plants (d), *ateiF3f-1/+* plants (e) and wild-type plants (f). The mutant pollen grains are labelled using GUS staining. Pt, pollen tube. (g) Pollen germination rates of *ateiF3f-1/+* and wild-type plants. Scale bars = 25 μ m.

mature pollen grains from *ateiF3f-1/+* plants, which contained 50% *ateiF3f-1* mutant pollen grains and 50% wild-type pollen grains, were also cultured *in vitro*. GUS staining showed that, of the cultured pollen grains, the mutant pollen

grains with GUS staining did not germinate or the pollen tube emerged but then stopped growing (Figure 1e), while the wild-type pollen grains without GUS staining produced a normal pollen tube (Figure 1f). Statistical analysis showed that only 40.2% of the pollen grains from *ateiF3f-1/+* plants (327/815) germinated *in vitro*, compared with 80.5% of the pollen grains from wild-type plants (317/394) (Figure 1g). These results indicate that the *ateiF3f-1* mutation strongly affects pollen germination and pollen tube growth.

The phenotype of *ateiF3f-1* is caused by a *Ds* insertion in *AtelF3f*

To determine the insertion site of the *Ds* element in *ateiF3f-1*, the flanking sequence containing the *Ds* 3' border sequence was obtained using thermal asymmetric interlaced PCR (TAIL-PCR) (Liu and Whittier, 1995; Liu *et al.*, 1995). Sequence analysis indicated that the *Ds* element was inserted in the 5' UTR of *At2g39990*, 13 bp downstream of the transcription start site and 70 bp upstream of the ATG (Figure 2a). This result was confirmed by PCR using gene-specific and *Ds* 5' border primers. The *Ds* insertion created a 6 bp (CGTCAG) duplication of the host sequence.

At2g39990 encodes a protein that contains the typical MPN (Mpr1/Pad1 N-terminal) domain conserved in eIF3f (see Figure S2) and has high similarity to the eIF3f proteins

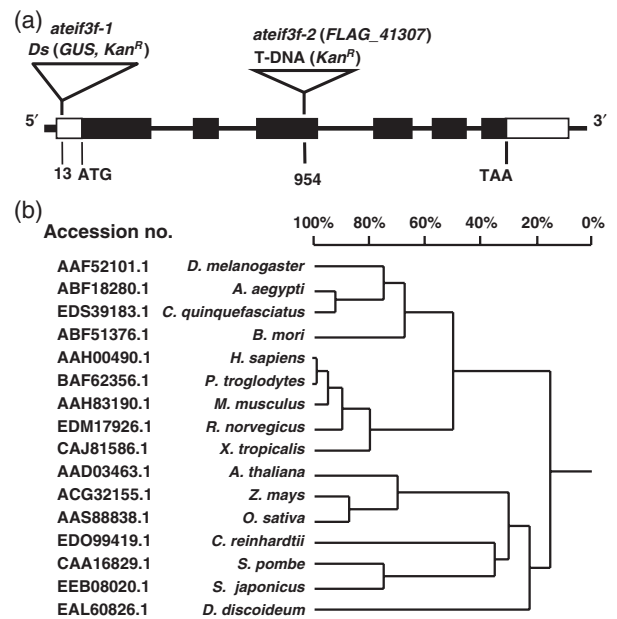


Figure 2. Characterization of the *AtelF3f* gene.

(a) The organization of the *AtelF3f* gene, showing the *Ds* element and T-DNA insertion sites. The black and white boxes indicate translated and untranslated regions, respectively.

(b) Phylogenetic tree of eIF3f proteins from 16 species created from the eIF3f sequences from GenBank using DNAMAN software (<http://www.lynnon.com>). The sequence identities between any two clusters or two genes can be determined by aligning the vertical lines of the tree with the percentage scale bar.

from human and yeast (Figure 2b). To confirm that the *ateif3f-1* mutant phenotype is caused by the *Ds* insertion in this gene, a 4.3 kb full-length genomic DNA fragment of *At2g39990*, including the promoter and 5' and 3' UTRs, was subcloned into the pCambia1300 vector. This construct was introduced into *ateif3f-1/+* plants. Transgenic lines were selected using kanamycin and hygromycin. The seeds from self-pollinated T₁ transgenic *ateif3f-1/+* plants were plated on kanamycin-containing agar plates to analyse the *Ds* segregation ratio. Most of the transformant lines (19 of 22) showed an elevated Kan^R:Kan^S segregation ratio of approximately 2:1. The complemented mutant plants produced progeny that were homozygous for the *ateif3f-1* mutation in T₂ and subsequent generations. When pollen grains from the two independent complemented lines homozygous for the *ateif3f-1* mutation were cultured *in vitro*, the germination rates increased to 74.9% (187/251) and 72.3% (175/244), close to the 80.3% (203/253) germination rate for wild-type pollen grains (Figure 3a–c). These results demonstrate that the defect in gametophytic function in *ateif3f-1/+* plants was fully complemented by full-length *At2g39990* (*AtelF3f*) genomic DNA.

We also examined the expression of *AtelF3f* in the *ateif3f-1* mutant using an *ateif3f-1/+* inflorescence RNA sample. The inflorescence transcriptome was mainly composed of the

gametophytic transcriptome, that was contributed by 50% wild type and 50% *ateif3f-1* mutant gametophytes. The real-time PCR results showed that expression of *AtelF3f* in the *ateif3f-1/+* inflorescences was greatly reduced compared to that in wild-type plants (Figure 3d). Therefore, expression of *AtelF3f* was knocked down in *ateif3f-1* mutant gametophytes.

To validate this result, *ateif3f-2* (*FLAG_41307*) was selected from the seed stocks of the *Arabidopsis thaliana* Resource Centre of the Versailles Genetics and Plant Breeding Laboratory (INRA, Paris, France). *ateif3f-2* is a T-DNA insertion mutant in *Arabidopsis* ecotype Wassilewskija (WS). PCR analysis using a T-DNA left-border primer and a gene-specific primer confirmed that T-DNA was inserted in the 3rd exon, 954 bp downstream of the ATG in *AtelF3f* (Figure 2a and Figure S2). The mutant also carried a Kan^R-selective marker. The progeny from self-pollinated *ateif3f-2/+* plants also exhibited a Kan^R:Kan^S segregation ratio of approximately 1:1 (1132:1348), instead of 3:1. When a wild-type *AtelF3f* full-length genomic DNA construct was introduced into *ateif3f-2/+* plants, 17 of 20 T₁ transgenic *ateif3f-2/+* lines showed an increased Kan^R:Kan^S segregation ratio of approximately 2:1. These findings are consistent with the results obtained from the study of *ateif3f-1/+* plants, and confirm that the defect in male gametophytes in *ateif3f-1* is caused by a mutation in *AtelF3f*.

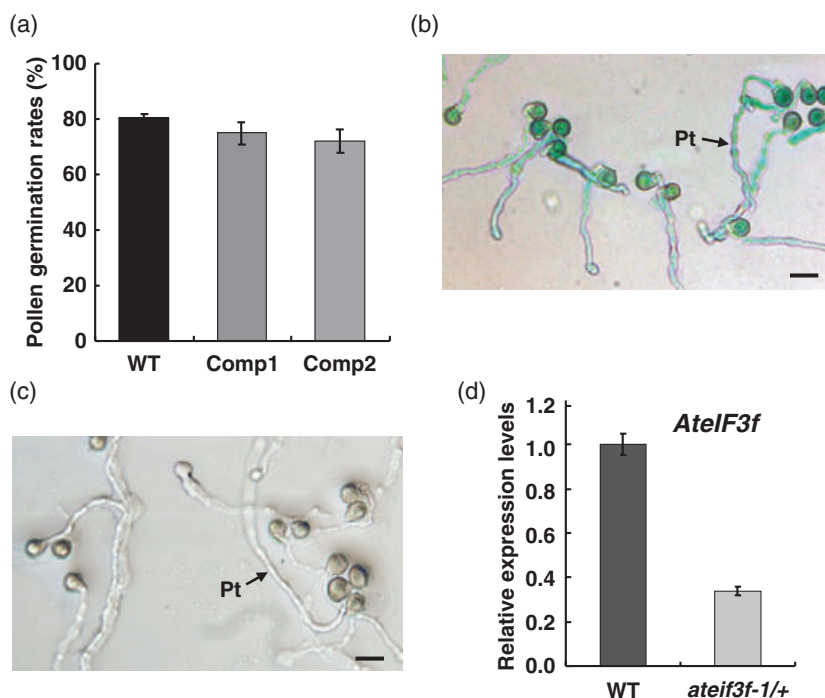


Figure 3. Complementation of the *ateif3f-1* mutant.

(a) Pollen germination rates of the complemented plants 1 (Comp1) and 2 (Comp2) homozygous for the *ateif3f-1* mutation.

(b,c) *In vitro* germination of pollen grains from *ateif3f-1* homozygous complemented lines (b) and wild-type plants (c). GUS staining indicates that the pollen grains carry the *ateif3f-1* mutation. Pt, pollen tube. Scale bars = 30 μ m.

(d) Expression level of *AtelF3f* in *ateif3f-1/+* flowers compared to that in wild-type plants.

AtelF3f is constitutively expressed, mostly in tissues active in cell growth and differentiation

To understand the function of *AtelF3f*, its expression pattern was assessed using RT-PCR with RNA isolated from various wild-type plant tissues. Expression of *AtelF3f* was detected in inflorescences, leaves, stems, siliques, roots and seedlings. Furthermore, the expression level of *AtelF3f* was different in the various tissues, with the highest level in inflorescences and the lowest level in stems (Figure 4a).

To investigate the expression pattern of *AtelF3f* in detail, a promoter fragment of *AtelF3f* was fused to a GUS reporter gene and introduced into wild-type plants. GUS activity was detected constitutively in many tissues, including pollen grains, embryos and root tips (Figure 4b–f).

The expression pattern of the AtelF3f protein was further investigated using an AtelF3f–GFP fusion protein construct under the control of the *AtelF3f* promoter (*pAtelF3f:AtelF3f-GFP*). The construct was introduced into the *ateif3f-1/+* mutant and wild-type plants. Phenotypic and genetic analysis showed that this construct complemented the phenotype of the *ateif3f-1/+* mutant (Table S1), indicating that the

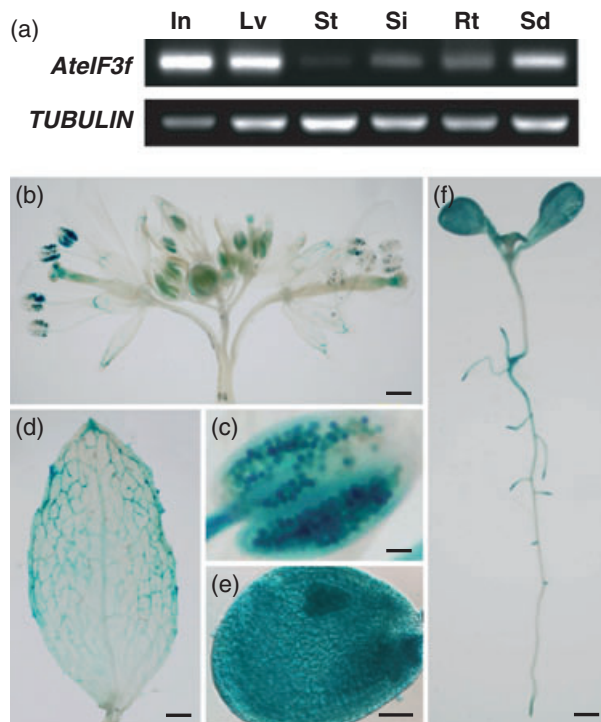


Figure 4. Expression pattern of *AtelF3f*. (a) RT-PCR assay comparing the *AtelF3f* mRNA levels in inflorescences (In), leaves (Lv), stems (St), siliques (Sd), roots (Rt) and seedlings (Si). The expression level of the *TUBULIN* gene was used as an internal control. (b–f) GUS activity in inflorescences (b), anthers (c), mature leaves (d), developing seeds (e) and seedlings (f) from transgenic wild-type plants carrying the *pAtelF3f:GUS* construct. Scale bars = 500 μ m (b,d,f) and 50 μ m (c,e).

AtelF3f–GFP fusion protein encodes a functional version of *AtelF3f*. GFP fluorescence was detected constitutively in many tissues, including the pollen grains, pollen tubes, embryos, ovules and root tips (Figure 5a–e). A magnified image of the GFP signal in a root tip cell showed that the fusion protein was localized in the cytoplasm (Figure 5f), which is consistent with the location of mRNA translation.

An *ateif3f-1* homozygous mutant generated by pollen rescue was defective in embryogenesis

To generate *ateif3f-1* homozygous plants for further investigation of *AtelF3f* function, we performed a pollen rescue experiment using promoters of the pollen-specific genes *VGD1* and *LAT52* (Muschiatti *et al.*, 1994; Jiang *et al.*, 2005) fused with *AtelF3f* cDNA. The resulting constructs, *pLAT52:AtelF3f* and *pVGD1:AtelF3f*, were introduced into *ateif3f-1/+* mutant plants to specifically rescue *ateif3f-1* pollen. Seeds from self-pollinated T₁ transgenic plants were plated on agar plates containing kanamycin. If the function of *ateif3f-1* pollen is fully recovered and the *ateif3f-1* homozygous seeds are able to grow normally, the Kan^R:Kan^S segregation ratio should increase to 2:1 according to Mendelian segregation. If the pollen function is fully complemented but the mutation causes embryonic lethality, the Kan^R:Kan^S segregation ratio should only increase to 1.5:1, and no *ateif3f-1* homozygous plants will be generated. The results showed that the Kan^R:Kan^S segregation ratio in the progeny from the pollen-rescued plants was approximately 1.5:1, consistent with the second hypothesis.

We investigated the embryogenesis process in pollen-rescued lines that were heterozygous for the *Ds* insertion and homozygous for the T-DNA insertion (*ateif3f-1/+ pLAT52:AtelF3f/pLAT52:AtelF3f* or *ateif3f-1/+ pVGD1:AtelF3f/pVGD1:AtelF3f*). In the siliques of these pollen-rescued plants, approximately 25% (151:627) of the seeds were defective (Figure 6a,c) compared to seeds from wild-type siliques (Figure 6b,d). The abnormal embryos stopped developing and started to degrade at various stages in different pollen-rescued lines. We randomly selected four transgenic lines, two from each construct, for further observation. In one transgenic line, the abnormal embryo stopped developing at the early globular stage (Figure 6e) and started to degrade when the normal embryos in the same silique were at the transition (globular to heart) stage (Figure 6f). In the other two transgenic lines, the mutant embryos developed to the late globular stage but were inflated and abnormal (Figure 6g), while the normal embryos in the same silique had developed to the torpedo stage (Figure 6h). In a few cases, the abnormal embryo survived (Figure 6i) until the normal embryos matured (Figure 6j). Some of the defective embryos developed into mature seeds and gave rise to seedlings on regular MS medium (Figure 7a). These seedlings had malformations in body shape, lacked chlorophyll and had abnormal

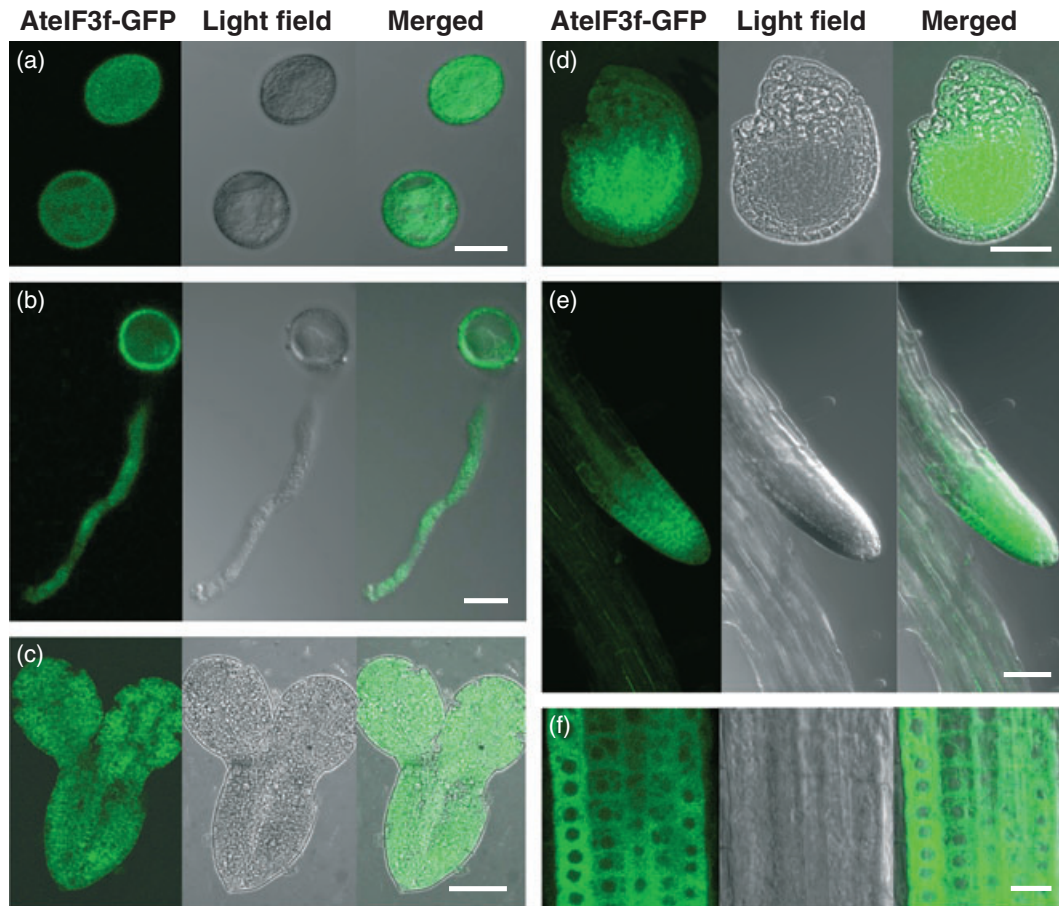


Figure 5. Expression of an *AtelF3f*-GFP fusion protein in various tissues. (a–f) GFP signals in mature pollen grains (a), pollen tubes (b), embryos (c), unfertilized ovules (d) and lateral root tips (e,f) from transgenic plants carrying the *pAtelF3f:AtelF3f-GFP* construct. Scale bars = 20 μm (a,b,f) and 50 μm (c–e).

anthocyanin accumulation, suggesting that their cell division and plastid differentiation processes were affected. Sometimes they even lacked hypocotyls and cotyledons (Figure 7b–d), and their root cell structure was severely disordered and disperse (Figure 7e). A PCR assay using DNA from the defective *ateif3f-1* seedlings indicated that they were homozygous for the *ateif3f-1* mutation. Real-time PCR and RT-PCR assays using RNA extracted from *ateif3f-1* homozygous seedlings showed that expression of *AtelF3f* was dramatically lower in such seedlings (Figure 7f,g). Transgenic wild-type plants with either *pLAT52:AtelF3f* cDNA or *pVGD1:AtelF3f* cDNA construct were also examined as negative controls. No defective embryos were found in these transgenic plants. Therefore, we conclude that the mutation in *ateif3f-1* leads to the embryo defect.

The *ateif3f-1* mutation affects the expression of genes related to cell development in Arabidopsis

Due to the limited supply of *ateif3f-1* homozygous plant material, we analysed the transcriptome alterations in

ateif3f-1 homozygous seedlings in comparison with wild-type seedlings using Affymetrix ATH1 genome arrays. Two biological replicates were performed, and the data from four ATH1 chips were analysed using affymGUI software (Wettenhall *et al.*, 2006). The expression of 3185 genes was changed more than threefold in *ateif3f-1* homozygous seedlings compared to wild-type seedlings (Appendices S1 and S2). The affected genes were involved in various biological processes, some of which are closely related to cell development. For example, *AtCSLA7* is required for normal pollen tube growth, embryo development and endosperm proliferation (Goubet *et al.*, 2003). The microarray result showed that the expression level of *AtCSLA7* in *ateif3f-1* homozygous seedlings was significantly lower than in wild-type seedlings (Figure 8a). This result was confirmed by real-time PCR and RT-PCR (Figure 8a,b).

Subunit eIF3h is involved in the sugar signalling pathway (Kim *et al.*, 2004), and so we looked particularly at sugar-sensing genes. We found that the expression levels of the sugar response genes *AT1G74670*, *ASPARAGINE*

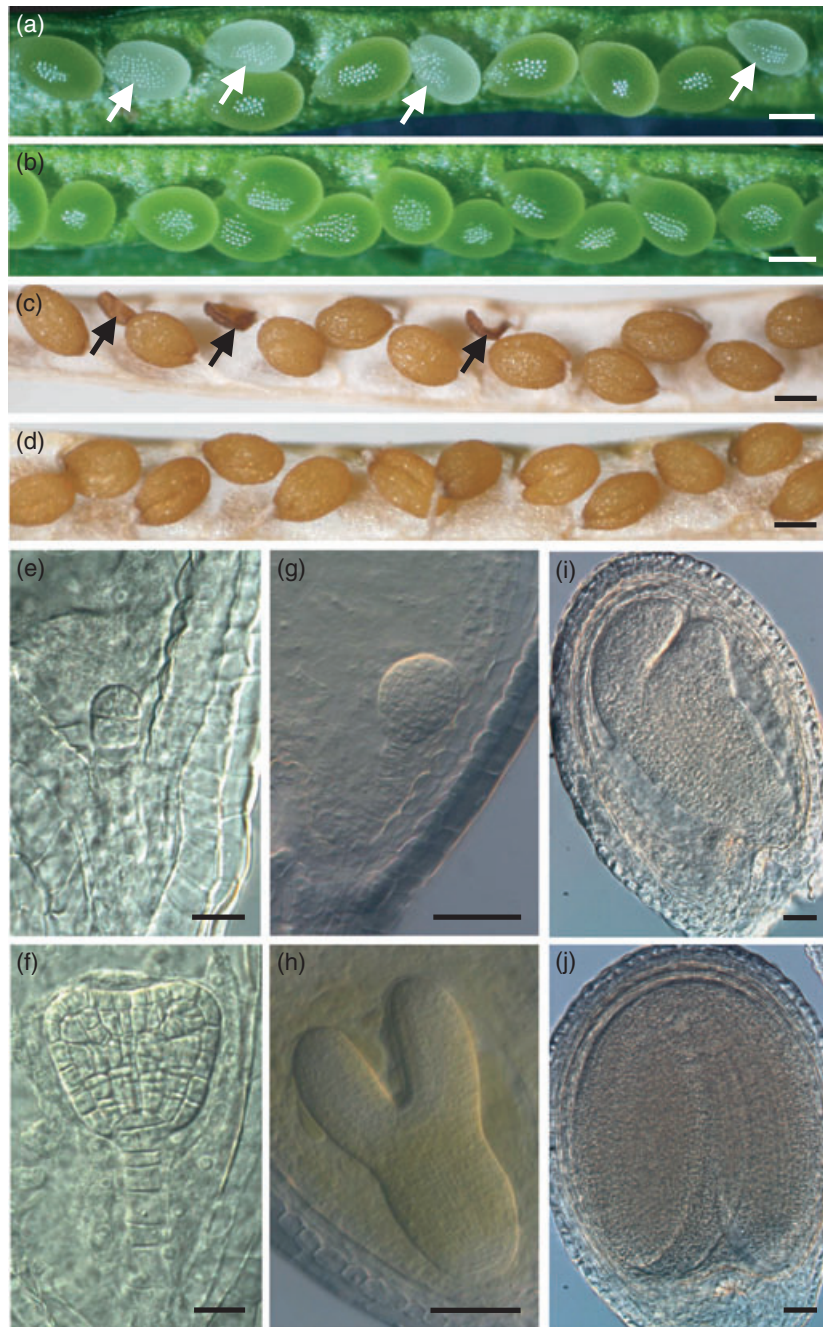


Figure 6. The mutation in *AtelF3f* affects embryo development.

(a,b) Developing siliques from wild-type plants (b) and *atelF3f-1/+* plants (a) carrying the pollen-rescuing construct *pVGD1:AtelF3f*, showing the white defective seeds (white arrows).

(c,d) Mature siliques from wild-type plants (d) and *atelF3f-1/+* plants (c) carrying the pollen-rescuing construct *pVGD1:AtelF3f* showing shrunken defective seeds (black arrows).

(e,g,i) *atelF3f-1* homozygous embryos from the pollen-rescued lines, arrested at the early globular (e), late globular (g) and torpedo (i) stages.

(f,h,j) Normal embryos in the same siliques as (e,g,i).

Scale bars = 200 μ m (a–d), 10 μ m (e,f) and 20 μ m (g–j).

SYNTHETASE1 (ASN1) and *PROLINE DEHYDROGENASE2 (ProDH2)* were reduced in the *atelF3f-1* homozygous seedlings to 1.4%, 2.4% and 25.3% of their levels in wild-type seedlings,

respectively (Figure 8c). The real-time PCR and RT-PCR assays confirmed that expression of *ASN1* was significantly reduced in *atelF3f-1* homozygous seedlings (Figure 8c,d).

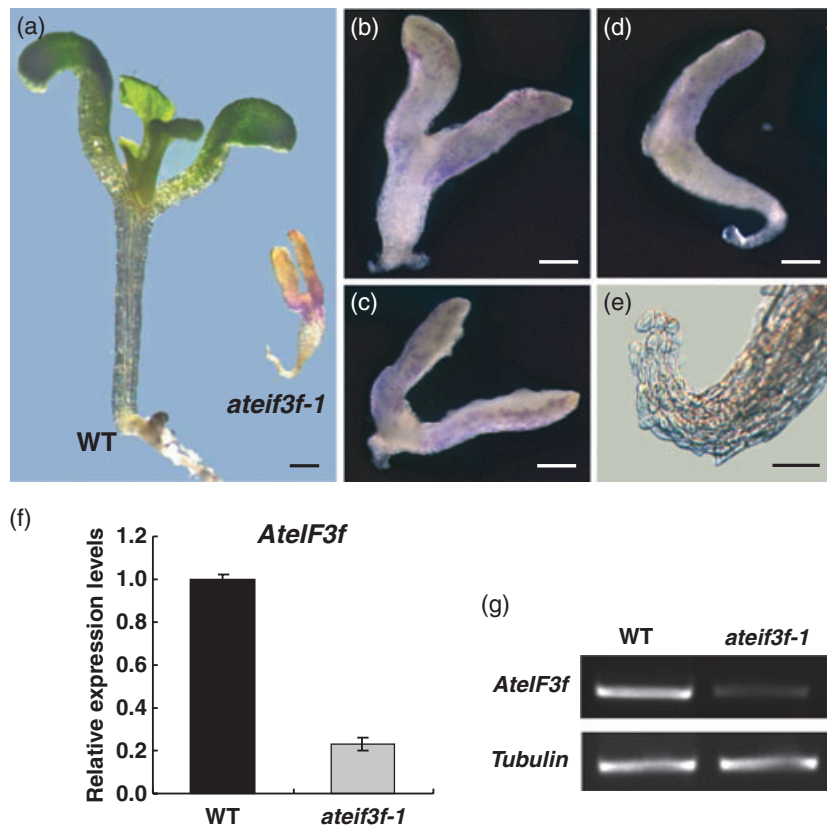


Figure 7. Characterization of *ateif3f-1* homozygous seedlings.

(a) Comparison of an *ateif3f-1* homozygous seedling and a normal wild-type seedling germinated under the same conditions.

(b–d) Phenotypes of *ateif3f-1* homozygous seedlings, showing that some lacked cotyledons (d) and some lacked hypocotyls and roots (c).

(e) Defective roots of *ateif3f-1* homozygous seedlings.

(f, g) Comparison of *AtelF3f* expression levels in wild-type seedlings and *ateif3f-1* homozygous seedlings by real-time PCR (f) and RT-PCR (g).

Scale bars = 200 μ m (a–d) and 100 μ m (e).

ateif3f-1 has phenotypes similar to those of *eif3h* and *eif3e* mutants

The mutation in *AtelF3f* may affect expression of sugar-sensing genes. To determine whether this was related to sugar responses, *ateif3f-1* seeds with the pollen-rescuing construct were germinated on MS agar plates containing 0%, 1%, 2%, 4% or 6% (W/V) sucrose. After culturing for 6 days under light, the *ateif3f-1* homozygous seedlings exhibited a sugar-sensitive phenotype, and grew best on medium without sucrose. Increasing sucrose concentrations may alter anthocyanin accumulation and repress chlorophyll synthesis (Figure 9a). Replacement of sucrose with glucose and maltose yielded similar results. When mannitol was substituted, however, the *ateif3f-1* homozygous seedlings synthesized chlorophyll at a similar level to that seen on the medium without any sugar (Figure 9b). This sugar-sensitive phenotype is similar to the phenotype of *eif3h-1* seedlings previously reported (Kim *et al.*, 2004).

To compare the *ateif3f-1* mutant with mutants for Arabidopsis *eIF3e*, *eif3e-1* (FLAG_495E05) was selected from the seed stocks of the *Arabidopsis thaliana* Resource Centre

(ARC) at the Versailles Genetics and Plant Breeding Laboratory (INRA, Paris, France). In *eif3e-1*, a T-DNA is inserted in the 4th intron, in the middle of the *eIF3e* gene. The T-DNA insertion also carries the Kan^R-selective marker. No *eif3e-1* homozygous mutant plants were identified in the progeny. When an *eif3e-1/+* plant was self-crossed, the Kan^R:Kan^S segregation ratio in the resulting progeny was approximately 0.73:1 (428:586) instead of the typical 3:1. When cultured *in vitro*, only 38.7% (210/543) of the pollen grains from *eif3e-1/+* plants germinated, compared to 78.8% (349/443) of the pollen grains from wild-type plants under the same conditions. These results showed that the mutation in the *eIF3e* gene also affects pollen germination, consistent with the results reported previously (Yahalom *et al.*, 2008). Therefore, the *ateif3f* mutant has similar phenotypes to those of *eif3e* and *eif3h* mutants in Arabidopsis.

AtelF3f protein interacts with the Arabidopsis regulatory subunit *eIF3e* and *eIF3h* in yeast and plant cells

As described above, the phenotypes of the *ateif3f* mutant were similar to those of *eif3e* and *eif3h*. *eIF3e* and *eIF3h* interact directly with each other in Arabidopsis (Kim *et al.*,

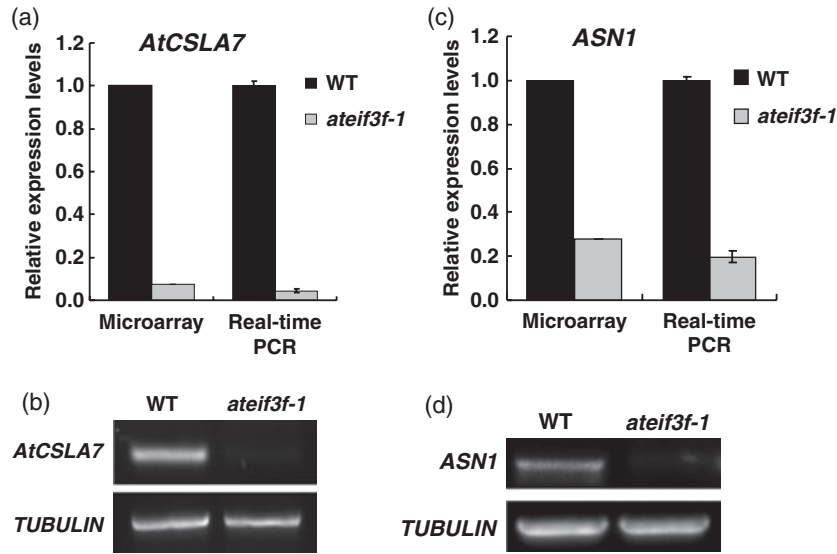


Figure 8. Mutation of *AtelF3f* affects the expression of downstream genes. Comparison of *AtCSLA7* and *ASN1* expression levels in *ateif3f-1* homozygous seedlings and wild-type seedlings using microarray data and real-time PCR (a,c) and RT-PCR (b,d).

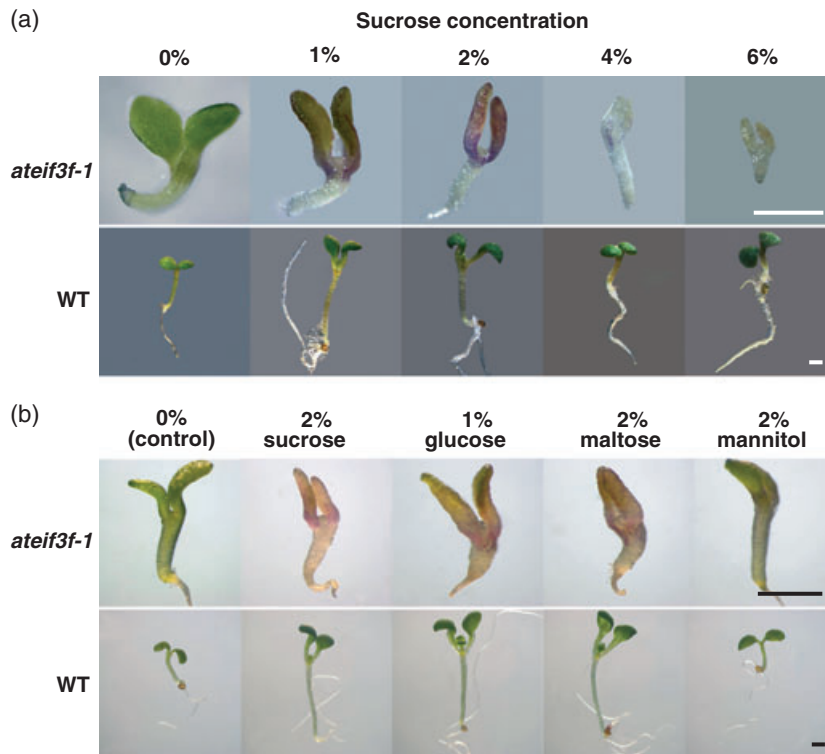


Figure 9. *ateif3f-1* homozygous seedlings are sensitive to exogenous sugars. (a) *ateif3f-1* homozygous and wild-type seedlings cultured on MS medium containing various concentrations of sucrose. (b) *ateif3f-1* homozygous and wild-type seedlings cultured on MS medium containing various sugars. Scale bars = 400 μm.

2004). These three subunits probably have a very close relationship to each other. To assess their connections further, we investigated the interaction among them using yeast two-hybrid (Y2H) assays. The coding regions of *eIF3e*

and *eIF3h* cDNAs from Arabidopsis were subcloned into the pGADT7 vector to generate target fusion protein constructs, while that of *AtelF3f* cDNA was subcloned into the pGBKT7 vector to generate a bait fusion protein construct.

Co-expression of these bait and target constructs showed that *AtelF3f* interacts with Arabidopsis eIF3e and eIF3h in yeast (Figure 10).

To support this result, a bimolecular fluorescence complementation (BiFC) assay was performed. The *AtelF3f* cDNA was subcloned into the vector pSPYNE-35S to generate a fusion protein with an N-terminus of yellow fluorescent protein (YFP) (*AtelF3f*-YN), and *eIF3e* and *eIF3h* cDNAs were subcloned into the vector pSPYCE-35S to generate the C-terminal YFP fusion proteins eIF3e-YC and eIF3h-YC. The constructs were introduced into an *Agrobacterium tumefaciens* strain. Pairs of strains expressing the *AtelF3f*-YN and *eIF3e*-YC constructs or the *AtelF3f*-YN and *eIF3h*-YC constructs were co-transformed into tobacco leaves. Four pairs of negative control strains were also used to transform the tobacco leaf cells. In transformed tobacco leaf cells, YFP fluorescence was detected in the cytoplasm when *AtelF3f*-YN and eIF3e-YC or *AtelF3f*-YN and eIF3h-YC were co-expressed (Figure 11a,b). No obvious fluorescent signal was detected by the expression of either *AtelF3f*-YN, eIF3e-

YC or eIF3h-YC alone (Figure 11c-f). This result shows that *AtelF3f* interacts with eIF3e and eIF3h in plant cells.

DISCUSSION

AtelF3f is important for normal cell growth and differentiation in Arabidopsis

In mammals, the subunit eIF3f is not essential for global translation initiation, but it has a wide range of roles in normal cell growth. For instance, eIF3f plays a central role in both the atrophic and the hypertrophic pathways in muscle cells. Genetic blockade of eIF3f expression induced atrophy. On the other hand, genetic activation of eIF3f promoted structural muscle protein synthesis and led to muscle hypertrophy (Csibi *et al.*, 2008). However, the roles of eIF3f in plant cells remain unknown. In this study, we found that a mutation in *AtelF3f* severely affected pollen germination and embryogenesis, providing evidence for an important role of *AtelF3f* in plant species. Transcriptome analysis of *ateif3f-1* homozygous seedlings showed that lack of *AtelF3f* significantly altered the expression of more than 3000 genes, many of which are important development-related genes, for example *AtCSLA7*. We verified that the expression of *AtCSLA7* was truly down-regulated in the mutant using real-time PCR. The expression of *AtCSLA7* was reduced to about 7% of the wild-type level in homozygous *ateif3f-1*

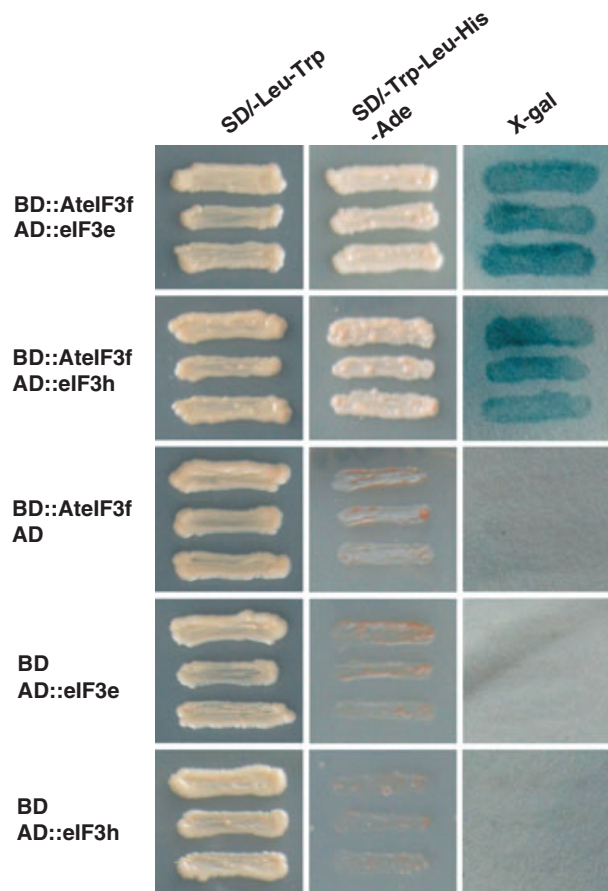


Figure 10. *AtelF3f* protein interacts with Arabidopsis eIF3e and eIF3h in yeast. Yeast cells carrying different constructs were cultured on SD/Leu-Trp medium and SD/Trp-Leu-His-Ade medium. The blue colour indicates activation of reporter genes. AD, target construct vector; BD, bait construct vector.

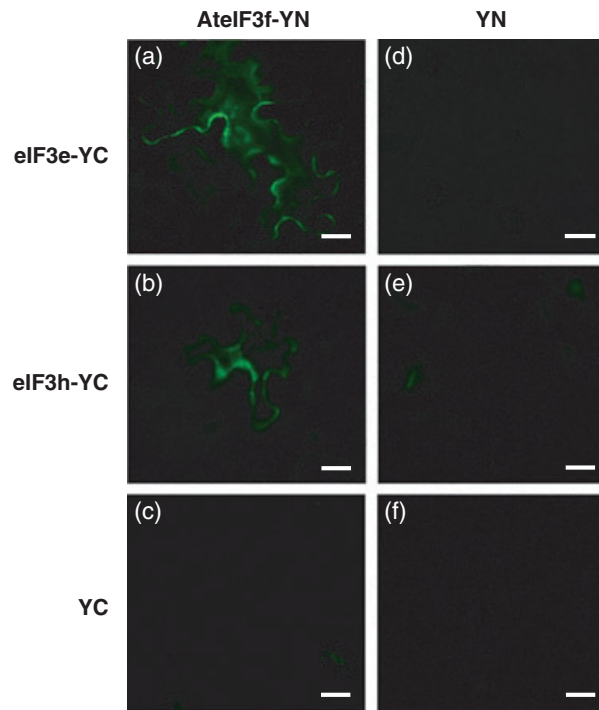


Figure 11. BiFC assay indicating that the *AtelF3f* protein interacts with Arabidopsis eIF3e and eIF3h in tobacco leaf cells. Co-expression of (a) *AtelF3f*-YN and eIF3e-YC, (b) *AtelF3f*-YN and eIF3h-YC, (c) YC and *AtelF3f*-YN, (d) YN and eIF3e-YC, (e) YN and eIF3h-YC, and (f) YC and YN. Scale bars = 30 μ m.

mutant seedlings (Figure 8a). *AtCSLA7* belongs to a sub-family of cellulose synthase-like (*CLS*) genes that are involved in biosynthesis of the plant cell wall. Mutation in *AtCSLA7* affected pollen tube growth and led to seed lethality (Goubet *et al.*, 2003). The microarray data also showed that *ASN1*, *SCO1*, *AtNAP7* and *CAO* were significantly down-regulated in the mutant seedlings. The expression level of *SCO1* was reduced to 14% of the wild-type level in homozygous *ateif3f-1* seedlings. Mutant *sco1* (*snowy cotyledon1*) embryos produce undifferentiated proplastids, resulting in defects in greening of the cotyledons of *sco1* seedlings (Albrecht *et al.*, 2006). The expression level of *AtNAP1* was reduced to 31% of the wild-type level in the *ateif3f-1* homozygous seedlings. The *AtNAP7* protein is localized in the plastid. Mutation of *AtNAP7* led to embryonic lethality at the globular stage. The *atnap7* mutant contained abnormally developing plastids with disorganized thylakoid structures (Xu and Moller, 2004). Expression of the *chlorophyllide a oxygenase* (*CAO*) gene, which regulates chlorophyll *b* synthesis, was reduced to 2.5% of the wild-type level in homozygous *ateif3f-1* seedlings (Espineda *et al.*, 1999; Yamasato *et al.*, 2008). In summary, these results imply that *AtelF3f* plays important roles in plant cell development, possibly by regulating the expression of genes important for normal pollen tube growth, embryo development, plastid differentiation and chlorophyll synthesis.

Our results show that *AtelF3f* interacts with eIF3h. The *ateif3f-1* mutant was hypersensitive to exogenous sucrose, similar to the *eif3h-1* mutant (Kim *et al.*, 2004, 2007). It has been reported that eIF3h is involved in translational initiation of transcription factor *ATB2/AtbZIP11* mRNA (Kim *et al.*, 2004, 2007). Previous studies proposed that *ASN1* and *ProDH2* were two direct targets of transcription factor *ATB2/AtbZIP11* in Arabidopsis (Hanson *et al.*, 2008) and the translation of *AtbZIP11* mRNA was repressed by sucrose (Rook *et al.*, 1998; Wiese *et al.*, 2004). Our microarray, real-time PCR and RT-PCR analyses all showed that the expression level of *ASN1*, the direct target of *AtbZIP11*, was drastically reduced in *ateif3f-1* homozygous seedlings (Figure 8c,d) (Hanson *et al.*, 2008). The microarray assay showed that expression of *AtbZIP11* at the transcriptional level was not reduced in *ateif3f-1* homozygous seedlings compared to wild-type seedlings. Thus, the *ateif3f-1* mutation did not affect the transcription of *AtbZIP11* mRNA. However, we still lack direct protein evidence for the effect of the *ateif3f-1* mutation on *AtbZIP11* mRNA translation due to a lack of *ateif3f-1* homozygous materials for protein preparation. Nevertheless, our results at least provide a clue that *AtelF3f* may affect the function of *AtbZIP11* in expression of *ASN1*.

In addition, *AtelF3f* was constitutively expressed at the highest level in actively growing tissues/cells such as pollen grains, pollen tubes, ovules, lateral root tips and embryos (Figures 4 and 5), implying that *AtelF3f* may be more

important in actively differentiating and proliferating tissues in Arabidopsis, such as the tissues involved in organ formation, than in other types of tissues. This assumption is consistent with the *ateif3f-1* mutant phenotypes observed in this study. For instance, the pollen tube growth of *ateif3f-1* was inhibited. In the pollen-rescued mutant lines, the *ateif3f-1* homozygous embryos were defective in organogenesis. Cotyledon and root formation were severely affected in some *ateif3f-1* homozygous seedlings. These results indicate that *AtelF3f* is important for normal plant cell growth, especially for cells undergoing differentiation and organ formation.

The activity of the eIF3 complex might be regulated by interaction partnerships between *AtelF3f*, eIF3e and eIF3h

eIF3 is structurally related to two other protein complexes, the COP9 signalosome (CSN) and the 19S proteasome lid. Most subunits of all three complexes contain one of two signature motifs, the PCI (proteasome/CSN/eIF3) domain or the MPN domain (Hofmann and Bucher, 1998). The subunits of the three complexes share sequence homologies with each other, and have a common 6 PCI + 2 MPN domain structure (Kim *et al.*, 2001; Chang and Schwechheimer, 2004; Scheel and Hofmann, 2005). Thus, subunits from one complex can interact with subunits from other complexes (Karniol *et al.*, 1998; Yahalom *et al.*, 2001; Kim *et al.*, 2004; Huang *et al.*, 2005). In Arabidopsis, previous studies have shown that eIF3h directly interacts with eIF3a, eIF3b, eIF3c, eIF3e, CSN7 and CSN8 (Kim *et al.*, 2004). The subunit eIF3e was purified together with the COP9 signalosome when it was first identified in plants (Karniol *et al.*, 1998). eIF3e also exhibited subcellular co-localization with CSN and was negatively regulated by CSN (Yahalom *et al.*, 2001, 2008). The multiple binding partnerships of eIF3e and eIF3h in Arabidopsis suggest that their activity might be regulated by these interacting proteins. In plant species, eIF3f has been identified from wheat and Arabidopsis eIF3 complexes. However, the interactive partners of eIF3f in plants remained unclear.

In this study, we demonstrated that *AtelF3f* interacts with both Arabidopsis eIF3e and eIF3h in Y2H and BiFC assays. Although the interaction partners of eIF3f are less well known in plant cells, several binding partners and a potential binding site of eIF3f have been identified in humans and yeast. For example, eIF3f is involved in apoptosis by interacting with cyclin-dependent kinase 11 (CDK11), which is an important effector in apoptosis (Shi *et al.*, 2003, 2009). Additionally, eIF3f interacts with coronavirus spike protein to inhibit host cell translation (Xiao *et al.*, 2008). eIF3f has also been reported to be a key target of the muscle-specific E3 ubiquitin ligase MAFbx/Atrogin-1 for ubiquitination and degradation by the proteasome during muscle atrophy (Csibi *et al.*, 2008). A possible binding site for mTOR (mammalian target of rapamycin) and S6K1 was found in the eIF3f subunit in mammals and yeast (Hinnebusch, 2006). The studies showed

that the TOR signalling network regulates the translation and transcription of ribosomal components, and revealed that S6K1 phosphorylates several targets related to translation. eIF3f mediates the association between the eIF3 complex and mTOR or S6K1, which switch the eIF3 complex on and off (Holz *et al.*, 2005; Harris *et al.*, 2006). These results imply the existence of many potential binding partners for AtelF3f in Arabidopsis.

The regulation of eIF3 activity might be tightly related to the protein interaction partners of AtelF3f, eIF3e and eIF3h. All the single mutants for AtelF3f, eIF3e and eIF3h have severe defects in plant cell growth, suggesting that the presence of the correct interacting partners of these subunits, including themselves, may be crucial for normal cell development.

EXPERIMENTAL PROCEDURES

Plant materials and growth conditions

The *Arabidopsis thaliana* plants used in this study were of the Landsberg *erecta* and Wassilewskija backgrounds. The plants were grown in soil at 22°C under a cycle of 16 h light/8 h dark. The generation of *Ds* insertion lines and the screening of mutants were performed as described by Sundaresan *et al.* (1995). The T-DNA insertion line, FLAG_41307, was obtained from the *Arabidopsis thaliana* Resource Centre (ARC) at the Versailles Genetics and Plant Breeding Laboratory (INRA, Paris, France).

Localization of *Ds* and T-DNA insertion sites in the *ateif3f* alleles

Isolation of the flanking sequences of the *Ds* element by TAIL-PCR (Liu *et al.*, 1995) was performed as described previously (Yang *et al.*, 1999) using *AtelF3f* genomic DNA and *Ds3/AD2* primer sets. The insertion site was confirmed by PCR using *Ds*-specific primers (*Ds*5-1, 5'-CCGTTTACCGTTTTGTATATCCCCG-3'; *Ds*5-2, 5'-CGTTCCGT-TTTCGTTTTTACC-3'; *Ds*5-3, 5'-GGTCGGTACGGGATTCCC-3') and the gene-specific primer 5'-CACCACCTATCCTTCGTAGAT-3'.

The T-DNA insertion site in the FLAG_41307 line was confirmed by PCR using the T-DNA left border-specific primer 5'-TCCGATTCAAGTACAATCGATT-3' and the gene-specific primer 5'-TTGATGCCCTTCTCCTACCTC-3'.

Characterization of pollen grains and pollen germination *in vitro*

Mature pollen grains were stained in a DAPI staining solution (0.1 M sodium phosphate, pH 7.0, 1 mM EDTA, 0.1% Triton X-100 and 0.25 mg ml⁻¹ DAPI). After incubation for 15 min, the stained pollen grains were viewed under UV light.

Pollen germination *in vitro* was performed as described by Jiang *et al.* (2005). The number of germinating pollen grains was counted after incubation at 22–24°C for 6 h.

Complementation experiments

A 4.3 kb full-length genomic DNA fragment of *AtelF3f* was amplified by PCR using primers 5'-AACTGCAGAGTCGTGACTCACTGAGTC-3' and 5'-ACGCGTCACTATGTTTCAGGACAGCTGACAT-3'. The resulting fragment was cloned into the pCAMBIA1300 vector and introduced into *ateif3f-1* and *ateif3f-2* heterozygous plants by the *Agrobacterium tumefaciens* (strain GV3101)-mediated infiltration method (Bechtold and Pelletier, 1998). Transformed plants were

selected on MS medium supplied with 50 mg L⁻¹ kanamycin and 20 mg L⁻¹ hygromycin.

The pollen rescue experiment was performed by pollen-specific expression of *AtelF3f* full-length cDNA in *ateif3f-1/+* plants. The *AtelF3f* full-length cDNA was amplified using primers 5'-GCTCTAGATTGATGCCTTCTCCTACCTC-3' and 5'-CGAGCTCCAACAAGAA-GCTGATTCTTAC-3'. The *LAT52* promoter fragment was obtained from the plasmid pUCLNGFP2 (a gift from Dr Zhenbiao Yang, Department of Botany and Plant Science, University of California at Riverside, CA). The *VGD1* promoter fragment was obtained from plasmid PME18 (Jiang *et al.*, 2005). The constructs were transformed into *ateif3f-1/+* plants.

The short cDNA fragment was amplified by PCR using primers 5'-GCTCTAGATTGATGCCTTCTCCTACCTC-3' and 5'-GGGGTACCTAGCATTGAGCAGCTGTGTT-3' to produce the *AtelF3f*-GFP fusion protein construct. The fusion protein was driven by the native *AtelF3f* promoter. The resulting constructs were transformed into *ateif3f-1/+* plants to examine whether the fusion protein was functional.

GUS assay

Pollen grains and vegetative tissues were stained in a 100 mM phosphate buffer solution (pH 7.0) containing 0.5 mM potassium ferricyanide [K₃Fe(CN)₆], 0.5 mM potassium ferrocyanide [K₄Fe(CN)₆], 0.1% Triton X-100, 10 mM EDTA and 0.5 mg ml⁻¹ bromochloroindoyl-β-glucuronide (X-Gluc). After incubation at 37°C overnight, the stained materials were clarified and observed as described by Jiang *et al.* (2005).

Microscopic observation of embryos

The embryos were treated in a clarifying solution for several minutes and observed using a Leica DM 2500 microscope (<http://www.leica.com/>). The clarifying solution contained 7.5 g gum arabic, 100 g chloral hydrate and 5 ml glycerol per 60 ml water.

RT-PCR and real-time PCR assays

Reverse transcription was performed using alfalfa mosaic virus reverse transcriptase (TaKaRa, <http://www.takara-bio.com>). *TUBULIN* cDNA was used as an internal control to normalize the amount of cDNA template. The primers 5'-CTTCGTATTTGGTCAATCCGGTGC-3' and 5'-GAACATGGCTGAGGCTGTCAAGTA-3' were used to amplify the *TUBULIN* cDNA fragment, and primers 5'-TTGTCGGC-TGGTATTCAACTG-3' and 5'-CGAGCTCCAACAAGAAGCTGATTCT-TAC-3' were used to analyse the *AtelF3f* expression levels in various tissues. The primers 5'-GTTAGGATGTTCCGATGATTCC-3' and 5'-AGGCTCATAAGGCGTTGAAGG-3' were used to assess the expression level of *ASN1*.

In real-time PCR assays, first-strand cDNA was synthesized using a SuperScript II kit (Invitrogen, <http://www.invitrogen.com/>). The expression levels of *AtelF3f*, *ASN1* and *AtCSLA7* were determined using Power SYBR Green PCR Master Mix on an ABI 7500 real-time instrument (Applied Biosystems (<http://www.appliedbiosystems.com/>)). The PCR program used was 95°C for 10 min, followed by 40 cycles of 95°C for 30 sec and 60°C for 1 min. The *18S rRNA* levels were quantified as an internal control to normalize the RNA quantity. The primers used to measure the expression levels of *AtelF3f*, *ASN1* and *AtCSLA7* are listed in Table S2. The relative mRNA levels were calculated by the comparative C_t method.

Microarray analysis

The RNA samples used in the microarray assay were extracted from wild-type and *ateif3f-1* homozygous seedlings. Two biological replicates were taken. ATH1 genome arrays (Affymetrix, [© 2010 The Authors
Journal compilation © 2010 Blackwell Publishing Ltd, *The Plant Journal*, \(2010\), **63**, 189–202](http://</p>
</div>
<div data-bbox=)

www.affymetrix.com) were used to assess the transcriptome differences between wild-type and *ateif3f-1* homozygous seedlings. The raw data (CEL files) for four ATH1 chips were analysed using affymGUI software (Wettenhall *et al.*, 2006). The genes whose expression was changed more than threefold were selected and grouped into down-regulated and up-regulated genes. More details of the microarray analysis are summarized in Appendices S1 and S2.

Yeast two-hybrid assay

The yeast two-hybrid assay was performed using Gal4 system vectors (Clontech, <http://www.clontech.com/>). The full-length coding sequences of Arabidopsis *eIF3e*, *AtelF3f* and *eIF3h* were amplified by PCR using the primers listed in Table S2. The *AtelF3f* cDNA fragment was cloned into the pGBKT7 vector, and the *eIF3e* and *eIF3h* cDNA fragments were cloned into the pGADT7 vector and co-transformed into yeast strain AH109.

BiFC assay

The coding sequences of Arabidopsis *eIF3e*, *AtelF3f* and *eIF3h* were amplified by PCR using the primers listed in Table S2. They were subcloned into vectors pSPYNE-35S and pSPYCE-35S (gift from Dr Shuhua Yang, College of Biological Sciences, China Agricultural University, Beijing, China) containing YFP fragments to form AtelF3f-YN, eIF3e-YC and eIF3h-YC fusion proteins. The constructs were introduced into *Agrobacterium tumefaciens* strain GV3101 by an electroporation method. The mixed strains were injected into 3-week-old tobacco leaves to transiently transform tobacco epidermal cells. Fluorescence was detected 3–6 days after infiltration.

ACKNOWLEDGEMENTS

This work was supported by research grants from the Ministry of Sciences and Technology (project numbers 2007CB108700 and 2007CB947600), the Natural Science Foundation of China (project number 30530060) and the Ministry of Education (111 project numbered B06003). We thank Dr V. Sundaresan (Department of Plant Sciences, University of California, Davis), Dr Wei-Cai Yang (Institute of Genetic and Development Biology, CAS, China) and Ms Li-Fen Xie (Temasek Life Sciences Laboratory, Singapore) for their kind help with the mutant screen.

SUPPORTING INFORMATION

Additional Supporting Information may be found in the online version of this article:

Figure S1. The *ateif3f-1* mutant expresses the GUS reporter.

Figure S2. Alignment of eIF3f protein sequences from six species.

Table S1. Genetic analysis of *pAtelF3f:AtelF3f-GFP* transgenic *ateif3f-1* mutant lines.

Table S2. Primers used in real-time PCR, Y2H and BiFC assays.

Appendix S1. Selected genes down-regulated in *ateif3f-1* homozygous seedlings.

Appendix S2. Selected genes up-regulated in *ateif3f-1* homozygous seedlings.

Please note: As a service to our authors and readers, this journal provides supporting information supplied by the authors. Such materials are peer-reviewed and may be re-organized for online delivery, but are not copy-edited or typeset. Technical support issues arising from supporting information (other than missing files) should be addressed to the authors.

REFERENCES

Albrecht, V., Ingenfeld, A. and Apel, K. (2006) Characterization of the *snowy cotyledon 1* mutant of *Arabidopsis thaliana*: the impact of chloroplast

elongation factor G on chloroplast development and plant vitality. *Plant Mol. Biol.* **60**, 507–518.

Asano, K., Kinzy, T.G., Merrick, W.C. and Hershey, J.W. (1997a) Conservation and diversity of eukaryotic translation initiation factor eIF3. *J. Biol. Chem.* **272**, 1101–1109.

Asano, K., Vornlocher, H.P., Richter-Cook, N.J., Merrick, W.C., Hinnebusch, A.G. and Hershey, J.W. (1997b) Structure of cDNAs encoding human eukaryotic initiation factor 3 subunits. Possible roles in RNA binding and macromolecular assembly. *J. Biol. Chem.* **272**, 27042–27052.

Asano, K., Phan, L., Anderson, J. and Hinnebusch, A.G. (1998) Complex formation by all five homologues of mammalian translation initiation factor 3 subunits from yeast *Saccharomyces cerevisiae*. *J. Biol. Chem.* **273**, 18573–18585.

Bandyopadhyay, A., Matsumoto, T. and Maitra, U. (2000) Fission yeast Int6 is not essential for global translation initiation, but deletion of int6(+) causes hypersensitivity to caffeine and affects spore formation. *Mol. Biol. Cell.* **11**, 4005–4018.

Bechtold, N. and Pelletier, G. (1998) *In planta* *Agrobacterium*-mediated transformation of adult *Arabidopsis thaliana* plants by vacuum infiltration. *Methods Mol. Biol.* **82**, 259–266.

Burks, E.A., Bezerra, P.P., Le, H., Gallie, D.R. and Browning, K.S. (2001) Plant initiation factor 3 subunit composition resembles mammalian initiation factor 3 and has a novel subunit. *J. Biol. Chem.* **276**, 2122–2131.

Chang, E.C. and Schwechheimer, C. (2004) ZOMES III: the interface between signalling and proteolysis. *EMBO Rep.* **5**, 1041–1045.

Chaudhuri, J., Chowdhury, D. and Maitra, U. (1999) Distinct functions of eukaryotic translation initiation factors eIF1A and eIF3 in the formation of the 40S ribosomal preinitiation complex. *J. Biol. Chem.* **274**, 17975–17980.

Csibi, A., Tintignac, L.A., Leibovitch, M.P. and Leibovitch, S.A. (2008) eIF3-f function in skeletal muscles: to stand at the crossroads of atrophy and hypertrophy. *Cell Cycle*, **7**, 1698–1701.

Dever, T.E. (2002) Gene-specific regulation by general translation factors. *Cell*, **108**, 545–556.

Doldan, A., Chandramouli, A., Shanias, R., Bhattacharyya, A., Cunningham, J.T., Nelson, M.A. and Shi, J. (2008a) Loss of the eukaryotic initiation factor 3f in pancreatic cancer. *Mol. Carcinog.* **47**, 235–244.

Doldan, A., Chandramouli, A., Shanias, R., Bhattacharyya, A., Leong, S.P., Nelson, M.A. and Shi, J. (2008b) Loss of the eukaryotic initiation factor 3f in melanoma. *Mol. Carcinog.* **47**, 806–813.

Dumas, C. and Gaude, T. (2006) Fertilization in plants: is calcium a key player? *Semin. Cell Dev. Biol.* **17**, 244–253.

Espineda, C.E., Linford, A.S., Devine, D. and Brusslan, J.A. (1999) The *AtCAO* gene, encoding chlorophyll *b* oxygenase, is required for chlorophyll *b* synthesis in *Arabidopsis thaliana*. *Proc. Natl Acad. Sci. USA*, **96**, 10507–10511.

Goubet, F., Misrahi, A., Park, S.K., Zhang, Z., Twell, D. and Dupree, P. (2003) AtCSLA7, a cellulose synthase-like putative glycosyltransferase, is important for pollen tube growth and embryogenesis in *Arabidopsis*. *Plant Physiol.* **131**, 547–557.

Hanson, J., Hanssen, M., Wiese, A., Hendriks, M.M. and Smeekens, S. (2008) The sucrose-regulated transcription factor bZIP11 affects amino acid metabolism by regulating the expression of ASPARAGINE SYNTHETASE1 and PROLINE DEHYDROGENASE2. *Plant J.* **53**, 935–949.

Harris, T.E., Chi, A., Shabanowitz, J., Hunt, D.F., Rhoads, R.E. and Lawrence, J.C. Jr (2006) mTOR-dependent stimulation of the association of eIF4G and eIF3 by insulin. *EMBO J.* **25**, 1659–1668.

Hinnebusch, A.G. (2006) eIF3: a versatile scaffold for translation initiation complexes. *Trends Biochem. Sci.* **31**, 553–562.

Hofmann, K. and Bucher, P. (1998) The PCI domain: a common theme in three multiprotein complexes. *Trends Biochem. Sci.* **23**, 204–205.

Holz, M.K., Ballif, B.A., Gygi, S.P. and Blenis, J. (2005) mTOR and S6K1 mediate assembly of the translation preinitiation complex through dynamic protein interchange and ordered phosphorylation events. *Cell*, **123**, 569–580.

Huang, X., Hetfeld, B.K., Seifert, U., Kahne, T., Kloetzel, P.M., Naumann, M., Bech-Otschir, D. and Dubiel, W. (2005) Consequences of COP9 signalosome and 26S proteasome interaction. *FEBS J.* **272**, 3909–3917.

Jiang, L., Yang, S.L., Xie, L.F., Pua, C.S., Zhang, X.Q., Yang, W.C., Sundaresan, V. and Ye, D. (2005) *VANGUARD1* encodes a pectin methyltransferase

- that enhances pollen tube growth in the Arabidopsis style and transmitting tract. *Plant Cell*, **17**, 584–596.
- Karniol, B., Yahalom, A., Kwok, S., Tsuge, T., Matsui, M., Deng, X.W. and Chamovitz, D.A. (1998) The Arabidopsis homologue of an eIF3 complex subunit associates with the COP9 complex. *FEBS Lett.* **439**, 173–179.
- Kawaguchi, R. and Bailey-Serres, J. (2002) Regulation of translational initiation in plants. *Curr. Opin. Plant Biol.* **5**, 460–465.
- Kim, T., Hofmann, K., von Arnim, A.G. and Chamovitz, D.A. (2001) PCI complexes: pretty complex interactions in diverse signaling pathways. *Trends Plant Sci.* **6**, 379–386.
- Kim, T.H., Kim, B.H., Yahalom, A., Chamovitz, D.A. and von Arnim, A.G. (2004) Translational regulation via 5' mRNA leader sequences revealed by mutational analysis of the Arabidopsis translation initiation factor subunit eIF3h. *Plant Cell*, **16**, 3341–3356.
- Kim, B.H., Cai, X., Vaughn, J.N. and von Arnim, A.G. (2007) On the functions of the h subunit of eukaryotic initiation factor 3 in late stages of translation initiation. *Genome Biol.* **8**, R60.
- Kolupaeva, V.G., Unbehauen, A., Lomakin, I.B., Hellen, C.U. and Pestova, T.V. (2005) Binding of eukaryotic initiation factor 3 to ribosomal 40S subunits and its role in ribosomal dissociation and anti-association. *RNA*, **11**, 470–486.
- Krichevsky, A., Kozlovsky, S.V., Tian, G.W., Chen, M.H., Zaltsman, A. and Citovsky, V. (2007) How pollen tubes grow. *Dev. Biol.* **303**, 405–420.
- Liu, Y.G. and Whittier, R.F. (1995) Thermal asymmetric interlaced PCR: automatable amplification and sequencing of insert end fragments from P1 and YAC clones for chromosome walking. *Genomics*, **25**, 674–681.
- Liu, Y.G., Mitsukawa, N., Oosumi, T. and Whittier, R.F. (1995) Efficient isolation and mapping of *Arabidopsis thaliana* T-DNA insert junctions by thermal asymmetric interlaced PCR. *Plant J.* **8**, 457–463.
- Lukaszewicz, M., Feuermann, M., Jerouville, B., Stas, A. and Boutry, M. (2000) *In vivo* evaluation of the context sequence of the translation initiation codon in plants. *Plant Sci.* **154**, 89–98.
- Malho, R., Liu, Q., Monteiro, D., Rato, C., Camacho, L. and Dinis, A. (2006) Signalling pathways in pollen germination and tube growth. *Protoplasma*, **228**, 21–30.
- Masutani, M., Sonenberg, N., Yokoyama, S. and Imataka, H. (2007) Reconstitution reveals the functional core of mammalian eIF3. *EMBO J.* **26**, 3373–3383.
- Muschiatti, J., Dircks, L., Vancanneyt, G. and McCormick, S. (1994) LAT52 protein is essential for tomato pollen development: pollen expressing antisense LAT52 RNA hydrates and germinates abnormally and cannot achieve fertilization. *Plant J.* **6**, 321–338.
- Nielsen, K.H., Szamecz, B., Valasek, L., Jivotovskaya, A., Shin, B.S. and Hinnebusch, A.G. (2004) Functions of eIF3 downstream of 48S assembly impact AUG recognition and GCN4 translational control. *EMBO J.* **23**, 1166–1177.
- Preuss, D., Rhee, S.Y. and Davis, R.W. (1994) Tetrad analysis possible in Arabidopsis with mutation of the *QUARTET (QRT)* genes. *Science*, **264**, 1458–1460.
- Ray, A., Bandyopadhyay, A., Matsumoto, T., Deng, H. and Maitra, U. (2008) Fission yeast translation initiation factor 3 subunit eIF3h is not essential for global translation initiation, but deletion of eif3h+ affects spore formation. *Yeast*, **25**, 809–823.
- Rook, F., Gerrits, N., Kortstee, A., van Kampen, M., Borrias, M., Weisbeek, P. and Smeeckens, S. (1998) Sucrose-specific signalling represses translation of the Arabidopsis *ATB2 bZIP* transcription factor gene. *Plant J.* **15**, 253–263.
- Scheel, H. and Hofmann, K. (2005) Prediction of a common structural scaffold for proteasome lid, COP9-signalosome and eIF3 complexes. *BMC Bioinformatics*, **6**, 71.
- Shi, J., Feng, Y., Goulet, A.C., Vaillancourt, R.R., Sachs, N.A., Hershey, J.W. and Nelson, M.A. (2003) The p34cdc2-related cyclin-dependent kinase 11 interacts with the p47 subunit of eukaryotic initiation factor 3 during apoptosis. *J. Biol. Chem.* **278**, 5062–5071.
- Shi, J., Kahle, A., Hershey, J.W., Honchak, B.M., Warneke, J.A., Leong, S.P. and Nelson, M.A. (2006) Decreased expression of eukaryotic initiation factor 3f deregulates translation and apoptosis in tumor cells. *Oncogene*, **25**, 4923–4936.
- Shi, J., Hershey, J.W. and Nelson, M.A. (2009) Phosphorylation of the eukaryotic initiation factor 3f by cyclin-dependent kinase 11 during apoptosis. *FEBS Lett.* **583**, 971–977.
- Sonenberg, N., Hershey, J.W.B. and Mathews, M. (2000) *Translational Control of Gene Expression*, 2nd edn. Cold Spring Harbor, NY: Cold Spring Harbor Laboratory Press.
- Sundaresan, V., Springer, P., Volpe, T., Haward, S., Jones, J.D., Dean, C., Ma, H. and Martienssen, R. (1995) Patterns of gene action in plant development revealed by enhancer trap and gene trap transposable elements. *Genes Dev.* **9**, 1797–1810.
- Valasek, L., Nielsen, K.H., Zhang, F., Fekete, C.A. and Hinnebusch, A.G. (2004) Interactions of eukaryotic translation initiation factor 3 (eIF3) subunit NIP1/c with eIF1 and eIF5 promote preinitiation complex assembly and regulate start codon selection. *Mol. Cell Biol.* **24**, 9437–9455.
- Wettenhall, J.M., Simpson, K.M., Satterley, K. and Smyth, G.K. (2006) affyGUI: a graphical user interface for linear modeling of single channel microarray data. *Bioinformatics*, **22**, 897–899.
- Wiese, A., Elzinga, N., Wobbes, B. and Smeeckens, S. (2004) A conserved upstream open reading frame mediates sucrose-induced repression of translation. *Plant Cell*, **16**, 1717–1729.
- Xiao, H., Xu, L.H., Yamada, Y. and Liu, D.X. (2008) Coronavirus spike protein inhibits host cell translation by interaction with eIF3f. *PLoS ONE*, **3**, e1494.
- Xu, X.M. and Moller, S.G. (2004) AtNAP7 is a plastidic SufC-like ATP-binding cassette/ATPase essential for Arabidopsis embryogenesis. *Proc. Natl Acad. Sci. USA*, **101**, 9143–9148.
- Yahalom, A., Kim, T.H., Winter, E., Karniol, B., von Arnim, A.G. and Chamovitz, D.A. (2001) Arabidopsis eIF3e associates with both eIF3c (INT-6) and the COP9 signalosome subunit CSN7. *J. Biol. Chem.* **276**, 334–340.
- Yahalom, A., Kim, T.H., Roy, B., Singer, R., von Arnim, A.G. and Chamovitz, D.A. (2008) Arabidopsis eIF3e is regulated by the COP9 signalosome and has an impact on development and protein translation. *Plant J.* **53**, 300–311.
- Yamasato, A., Tanaka, R. and Tanaka, A. (2008) Loss of the N-terminal domain of chlorophyllide *a* oxygenase induces photodamage during greening of Arabidopsis seedlings. *BMC Plant Biol.* **8**, 64.
- Yang, W.C., Ye, D., Xu, J. and Sundaresan, V. (1999) The *SPOROCTELESS* gene of Arabidopsis is required for initiation of sporogenesis and encodes a novel nuclear protein. *Genes Dev.* **13**, 2108–2117.
- Zhou, C., Arslan, F., Wee, S., Krishnan, S., Ivanov, A.R., Oliva, A., Leatherwood, J. and Wolf, D.A. (2005) PCI proteins eIF3e and eIF3m define distinct translation initiation factor 3 complexes. *BMC Biol.* **3**, 14.
- Zhou, M., Sandercock, A.M., Fraser, C.S. et al. (2008) Mass spectrometry reveals modularity and a complete subunit interaction map of the eukaryotic translation factor eIF3. *Proc. Natl Acad. Sci. USA*, **105**, 18139–18144.